医薬品研究
Pharm. Regul. Sci.
40(12)848～852(2009)

品質に関するトピックの動向
Q-IWG：品質実施作業部会**

檜山行雄*

1. はじめに

本稿ではQ8，Q9及びQ10のImplementation Working Groupについて報告します．

グループの活動目的は，Q8，Q9及びQ10の一貫した導入と実践を世界的に行うこと及び，この三つのガイドラインを相乗効果でより大きい成果を上げることです（Table 1）．グループが組織された背景として，2003年のブラッセル会議が起点となります．その後，製剤開発（Q8），品質リスクマネジメント（Q9），医薬品品質システム（Q10）が作成されました．これらガイドラインは，概念的であり，今後の方針に関わることが多く，またなじみのない概念も含まれていました．これらの内容を明確にして，曖昧さや不確定さを取り除くことが背景になっています（Table 2）．

2006年のQuality Strategy Meetingでは，Q8，Q9及びQ10の導入・実践に関しては今後注意深く，ある程度精密に作業を行っていかなければその実現は難しいという認識がされました．2007年になり，非公式のQ-IWGが開催され，その後，3回のface-to-face MeetingがIWGとして行われ，2009年6月に横浜で3回目のQ-IWGが開催されました（Table 3）．

2. Q-IWGの検討課題と運営

検討課題は，審査と査察の領域を対象に，用語の共通理解，Q8，Q9及びQ10のガイドラインの相互関係の理解を進めることです．また導入後，申請資料の中にどの様に書き込むのかといった調和の程度も課題として取り上げます．Q8，Q9及びQ10の導入・実践を行った場合に，今まで作成されたICHのQualityガイドラインに何らかの影響が及ぶことが考えられるので，それらの課題を洗い出して対応していきます．

また，Q8，Q9及びQ10ガイドラインに関するコミュニケーションとトレーニングを行います．具体的には，Q＆Aや教育資料を作成する，外部団体と共同作業を行う，ワークショップを開くことなどです．

具体的なQ-IWGの運営は，当初，Quality by Design，知識管理，医薬品品質システム・査察の三つの領域について，IWGの成果物である，Q＆A，White papers，Position papersや事例の作成，ワークショップ開催などを実行することです．

またIWGでは，ICHのweb siteを通してIWGに対する提案を受け付けます．Q＆AのQuestionsとAnswersをセットでも，Questionsだけでも，提案を受け付けます．また，外部の非営利団体との共同作業を行う予定です（Table 4）．

2008年のポートランド会議で，先の三つの領域で分科会を設け，Brain Stormingを行いました．その結果得られた課題について，知識管理は日本，Quality by Designはアメリカ，Pharmaceutical Quality System/Inspectionは欧州がそれぞれ担当して，具体的なQ＆Aの作成を行いました．また，外部団体との共同作用についても議論をしました．

2008年秋のブラッセルでは，分担して作成した各領域のQ＆Aを持ち寄り，face-to-faceの会議で40以上を採択しました．その後，会議で合意したQ＆Aは各極でreviewし，2009年3月の電話会議

* 国立医薬品食品衛生研究所薬品部　東京都世田谷区上用賀1-18-1（〒158-8501）
** 当協会主催の第20回ICH即時報告会（平成21年6月12日：東京）における講演による．

Table 1 Objectives

- Globally consistent implementation of Q8, Q9 and Q10
- Maximum benefit from the interaction between the guidelines

Final Concept Paper , ICH IWG on Q8, Q9 and Q10, November1, 2007
http://www.ich.org/LOB/media/MEDIA4457.pdf

Table 2 Background

- In Brussels 2003 a new quality vision was agreed on. emphasising a risk and science-based approaches to pharmaceuticals in an adequately implemented quality system.
- As a consequence, Pharmaceutical Development (Q8),Quality Risk Management(Q9)
- and Pharmaceutical Quality System(Q10) were drafted.
- Because concepts and principles are rather new, it is important to provide clarity/further explanation and to remove ambiguities and uncertainties.

Table 3 History

- Quality Strategy Meeting, Fall 2006 Chicago
- Quality Strategy Meeting, Spring 2007 Brussels
- Quality Satellite Roundtable, Fall 2007 Rockville
- Informal Q-IWG, October 2007 Yokohama
  - Final Concept Paper endorsed by Steering Committee
- First Q-IWG Meeting, June 2008 Portland
  - Three breakout sessions on Knowledge Management, Quality by Design, Pharmaceutical Quality System/Inspection.
- Second Q-IWG Meeting, November 2008 Brussels
  - More than 40 Q&A's agreed by IWG. Feedback collected.
- Teleconference on March 11, 2009
  - 30 Q&A's adopted
- Third Q-IWG Meeting, June 2009 Yokohama

で最終的に30件のQ&Aを採択しました．このQ&AはICHのweb siteに掲載されています（Table 5）．

3. ガイドライン理解のためのQ&A

Q&Aを紹介します．Quality by Designのセクションの Real Time Release Testingの採用により，バッチの出荷判断にどのような影響があるかとの質問です（Table 6）．

Table 4 Q IWG operation

- Areas of Topics
  - Quality by Design, Knowledge Management, Pharmaceutical Quality System/Inspection
- Outcome/Product from IWG
  - Q&As
  - White papers
  - Examples and Case studies
  - Training, Workshops
- Work processes/Collaborations
  - Within IWG
  - Proposals to IWG at the following ICH Q-IWG web site (http://www.ich.org/cache/html/5050-272-1.html)
  - Collaborations with non-profit organizations

Table 5 Progress in and after Brussels meeting

- More than 40 draft QA's were agreed
- Regional review of draft QA's
- 30 QA's were adopted at telecon on March 11, 2009 (http://www.ich.org/LOB/media/MEDIA5290.pdf)

Batch releaseというの市場への出荷時の最終的な判断で，Real Time Release Testingを行うか，品質の試験，つまり規格の試験をするかに関わらず，Batch releaseは行われます．回答には，GMP下で行われる通常の出荷の判断の基本的なことが書いてありますが，Real Time Release Testingの議論は，ICHのQ8(R1)に定義されています．ところが，実際の生産現場はGMPに沿って作業は行われます．すなわち，一つのガイドラインで規定したことが，他のpracticeに少なからず影響を及ぼします．この例はGMP下での出荷に影響する部分ですから，このようなQ&Aを出して明確化を図るということです．

Table 6 2. Quality by Design: 2.2 Real Time Release Testing

Q 01: How is batch release affected by employing real time release testing?
A: Batch release is the final decision to release the product to the market regardless whether RTR testing or end product testing is employed. End product testing involves performance of specific analytical procedures on a defined sample size of the final product after completion of all processing for a given batch of that product. Results of real time release testing are handled in the same manner as end product testing results in the batch release decision. Batch release involves an independent review of batch conformance to predefined criteria through review of testing results and manufacturing records together with appropriate GMP compliance and quality system, regardless of which approach is used.

Table 7は医薬品品質システムの導入 に関するQ&Aを，Table 8には，GMP査察へのインパクトに関するのQ&Aの一例を示します．

Table 9は，ICH Q8，Q9及びQ10の発効により，知識管理の重要度と使い方はどのように変わるのか，あるいはどのように変わったのか，という質問です．

Q10には，知識管理の定義が収載され，「製品，製造プロセス，及び構成資材の情報を獲得，分析，保管，伝播するための体系的な取り組み」とされています．知識管理は新しい概念ではなく，Q8，Q9及びQ10の発効に関わらず重要です．ただ，Q10では，最近のいわゆるenhanced approach，Quality

Table 7 3. Pharmaceutical Quality System

Q 01: What are the benefits of implementing a Pharmaceutical Quality System (in accordance with ICH Q10)?
A: The benefits are:
· Facilitated robustness of the manufacturing process, through facilitation of continual improvement through science and risk-based post approval change processes.
· Consistency in the global pharmaceutical environment across regions
· Enable transparency of systems, processes, organisational and management responsibility.
· Clearer understanding of the application of a Quality System throughout product lifecycle.
· Further reducing risk of product failure and incidence of complaints and recalls thereby providing greater assurance of pharmaceutical product consistency and availability (supply) to the patient.
· Better process performance.
· Opportunity to increase understanding between industry and regulators and more optimal use of industry and regulatory resources. Enhance manufacturer's and regulators' confidence in product quality.
· Increased compliance with GMPs, which builds confidence in the regulators and may result in shorter inspections.

Table 8 4. ICH new quality guidelines' impact on GMP inspection practices

Q01: How will product-related inspections differ in an ICH Q8, Q9 and Q10 environment?
A: In the case of product-related inspection (in particular pre-authorisation) depending on the complexity of the product and/or process, there could be a need for greater collaboration between inspectors and assessors for example for the assessment of development data. The inspection would normally occur at the proposed commercial manufacturing site and there is likely to be greater focus on enhanced process understanding and understanding relationships e.g. Critical Quality Attribute (CQAs), Critical Process Parameters (CPPs). It will also extend into the application and implementation of quality risk management principles, as supported by the Pharmaceutical Quality System (PQS).

Table 9 5. Knowledge Management

Q 01: How has the implementation of ICH Q8, Q9, and Q10 changed the significance and use of knowledge management?
A: Q10 defines knowledge management as: 'Systematic approach to acquiring, analyzing, storing, and disseminating information related to products, manufacturing processes and components'.
Knowledge management is not a system; it enables the implementation of the concepts described in ICH Q8, Q9 and Q10.
Knowledge Management is not a new concept. It is always important regardless of the development approach. Q10 highlights knowledge management because it is expected that more complex information generated by appropriate approaches (e.g. QbD, PAT, real-time data generation and control monitoring systems) will need to be better captured, managed and shared during product life-cycle. . In conjunction with Quality Risk Management, Knowledge Management can facilitate the use of concepts such as prior knowledge (including from other similar products), development of design space, control strategy, technology transfer, and continual improvement across the product life cycle.

by Design, あるいは process analytical technology を採用した場合の知識管理は，より複雑な内容を扱うので，より知識管理の重要度が上がると回答では記述されています．

もともと Knowledge Management は Q10 で定義され，説明されていますが，Q8 の中でいわれている enhanced approach を実際の現場で運用するときに，enhanced approach の知識をどのように保存して，どのように site に供給していくかと回答には示してあります．

4. 横浜会議での Q-IWG の成果

横浜では大きく分けて三つの領域で議論が行われました．

Q&A については追加が議論され，その結果，10 件の Q&A が新たに採択されました．

新しく採用された 10 件の一つを紹介します (Table 10)．これは製造所では，どんな製剤開発の情報や文書が必要かという質問です．医薬品開発情報は通常，開発部門で利用できる状態であるべきです．製剤開発から入る情報は，製造あるいは製造管理に必要な重要な情報なため，製造部門で活用できる状態になければならないと回答されています．そのことが技術移転を成功させる鍵になると述べています．

Case Studies を採択するためには，外部論文を review して引用するには，多くの労力が必要となるため断念しました．それに代わり，IWG 自身が外部団体と共同で Position Papers や White Papers を書くことになり，Task force を作り，今後取り組みます (Table 11)．

トレーニングは，Q8，Q9 及び Q10 の implementation を世界中で行うために実施します．Q-IWG が主体となったワークショップの開催を提案し，運営委員会で承認されました．Table 12 にワークショップの達成目標を示します．Q8，Q9 及び Q10 と Q&A を取り込み，製品のライフサイクルに合わせ，全般にわたってトレーニング・プログラムを組む計

Table 10 2. Pharmaceutical Quality System

Qxx: What information and documentation of the development studies should be available at a manufacturing site?
A: Pharmaceutical development information (e.g. supporting information on design space, chemometric model, risk management,…) is available at the development site.
Pharmaceutical development information which is useful to ensure the understanding of the basis for the manufacturing process and control strategy, including the rationale for selection of critical process parameters and critical quality attributes should be available at the manufacturing site.
Scientific collaboration and knowledge sharing between pharmaceutical development and manufacturing is essential to ensure the successful transfer to production.

Table 11 Case Studies (Articles / Position Papers)

- Q-IWG findings
  - Many publications, workshops etc. available
  - Q-IWG will not endorse existing articles
    - Resource intensive: reviewing, decision, maintenance etc.
    - Potential regulatory concerns
  - Q-IWG will initiate, encourage and collaborate on paper development consistent with Q8, Q9, Q10 guidelines and Q&A
- How can this be achieved?
  - Task force within Q-IWG
    - Identification of topics and potential collaborators
    - Establish process for outside contribution
    - Recommend the topic and potential collaborators to Q-IWG
  - Q-IWG to assign topic cordinator(s) among its members
  - Final review and approval by entire Q-IWG (e.g. by telecon)

Table 12 Training / Workshops: Goals and objectives

- Enhanced harmonised implementation training to industry and regulators at the three ICH regions
- Conducted by ICH experts, who developed the guidelines and members of the ICH Quality Implementation Working Group (Q-IWG)
- The only workshops endorsed by the ICH Q-IWG and conducted by the same faculty in all three ICH regions.
- The training will cover the integrated use of the ICH Q8, Q9 and Q10 guidelines and Q&A across the product life cycle, from development to manufacturing and commercialisation

Table 13 Proposed additional activities

- Identifying the need of revision / update of existing ICH Quality guidelines in the context of ICH Q8, Q9, Q10 and pending Q11
- Other evolving topics impacted and stimulated in the light of the new paradigm to be identified for avoiding potential disharmonisation
- Proposal to revise the Q-IWG mandate will be presented in ICH St. Louis

画です．トレーニングの対象は企業関係者だけではなく，行政の審査や監視の担当者を含めて行う予定です．

計画の概要は，講義を半日，分科会を1日，パネルディスカッションを半日ぐらいの正味2日の計画を検討しています．開催時期は，欧州は2010年のブラッセル会議に，日本では2010年秋の横浜会議前に，アメリカではその間あたりを予定しています．

5. おわりに（Table 13）

今後，Q8からQ10までを導入することで，既存のQualityガイドラインに影響を与えることになり，そのためどのような問題が発生するかを検証し，手当てを行う予定です．

また，新たに多くの技術や考え方が出てくるので，それらをどのように扱うか，IWGで議論していきます．今までにQ-IWGがカバーしてきたのは，Q10と最後にStep 4に達したQ8(R1)です．その後，約1年でQ-IWGの活動は終了すると提案されていましたが，少し新しいタスクを加えることで活動が延長されることになります．今後の活動経過はセントルイス会議において運営委員会へ提案をすることになります．

Division of Drugs[1], National Institute of Health Sciences, Tokyo, Japan; TeraView Limited[2], St John's Innovation Park, Cambridge, United Kingdom; TDDS Research Laboratory[3], Hisamitsu Pharmaceutical Co. Inc., Tsukuba; Bruker Optics K.K[4], Tokyo, Japan

Detection of tulobuterol crystal in transdermal patches using Terahertz pulsed spectroscopy and imaging

T. Sakamoto[1], A. Portieri[2], P. F. Taday[2], Y. Takada[3], D. Sasakura[4], K. Aida[3], T. Matsubara[4], T. Miura[4], T. Terahara[3], D. D. Arnone[2], T. Kawanishi[1], Y. Hiyama[1]

Received January 19, 2009, accepted February 21, 2009

Dr. Tamoaki Sakamoto, Division of Drugs, National Institute of Health Sciences, 1-18-1, Kami-yoga, Setagaya-ku, Tokyo 158-8501, Japan
tsakamot@nihs.go.jp

Pharmazie 64: 361–365 (2009) *doi: 10.1691/ph.2009.9022*

Applicability of a Terahertz Pulsed Spectroscopy (TPS) and a Terahertz Pulsed Imaging (TPI) for detection of tulobuterol (TBR) crystals in transdermal patches was investigated. Because TBR has high permeability in dermis, crystalline TBR in patch matrices contributes to controlling the release rate of TBR from a matrix. Therefore, crystalline TBR is one of the important factors for quality control of TBR transdermal tapes. A model tape that includes 5 w/w%, 10 w/w%, 20 w/w% or 30 w/w% of TBR was measured by TPS/TPI. TBR crystals in the matrices were successfully detected by TPI. Identification of TBR in an image of a crystal-like mass was done by comparison between the spectra of tapes and a TBR standard substance. These results indicate that TPS and TPI are applicable to identifying crystalline lumps of an active drug in tapes for quality control.

1. Introduction

Terahertz (THz) time-domain spectroscopy gives an electric field record of time delay due to the presence of material in a beam path with a higher refractive index when compared to a reference. Fourier-transformed waveforms from an electric field show a characteristic relationship between frequency and absorbance. Fourier-transformed waveforms provide information about not only intra-molecular vibration and lattice vibration, but also intermolecular forces and hydrogen bonds.

In the pharmaceutical industry, applications of TPS and TPI for discrimination of polymorphs (Taday et al. 2003; Walther et al. 2003; Strachan et al. 2004, 2005; Zeitler et al. 2005, 2006, 2007, Day et al. 2006) and for detecting unique waveforms of APIs have been reported. Thus, these technologies are expected to be used for qualitative and/or quantitative analysis (Taday et al. 2003; Upadhya et al. 2003; Ueno et al. 2006; Zeitler et al. 2006). In particular, THz spectroscopy has been used for detecting foreign materials in samples and for measuring the thickness of coatings (Fitzgerald et al. 2005; Zeitler et al. 2006; Ho et al. 2007).

Tulobuterol ((*R,S*)-2-tert-butylamino-1-(2-chlorophenyl) ethanol, TBR) transdermal tapes are used to cure bronchial asthma as a bronchodilator (β_2-blocker). TBR is one of the suitable compounds for systemic transdermal formulation because it has very high permeability into the keratin layer. The release rate of TBR from the matrix is controlled by the formation of lumps of TBR crystals. For this reason, crystallization of TBR in a matrix is an important factor assuring the quality of this tape. However, verifying the crystallization of an active drug is difficult because TDDS tapes (or patches) generally have a sandwich-like structure with a matrix between a liner and a supporting board. Although release testing is often used to evaluate "releasability", which is one of the physico-chemical properties of an active drug in transdermal pharmaceuticals, releasability is not a suitable parameter for evaluating crystallization of an active drug. In order to compensate for this disadvantage, development of an alternative method by which to observe crystallization of an active drug in a matrix through a liner and/or a supporting board is needed. This manuscript describes the applicability of one of the innovative non-destructive analytical techniques, TPS and TPI, for quality evaluation of TDDS tapes.

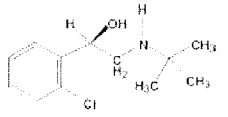

Tulobuterol

2. Investigations, results and discussions

2.1. THz pulsed spectrum of TBR obtained by TPS instrument

Fig. 1(A) shows the typical THz electric field records obtained from the TBR pellet and reference (PE pellet) by

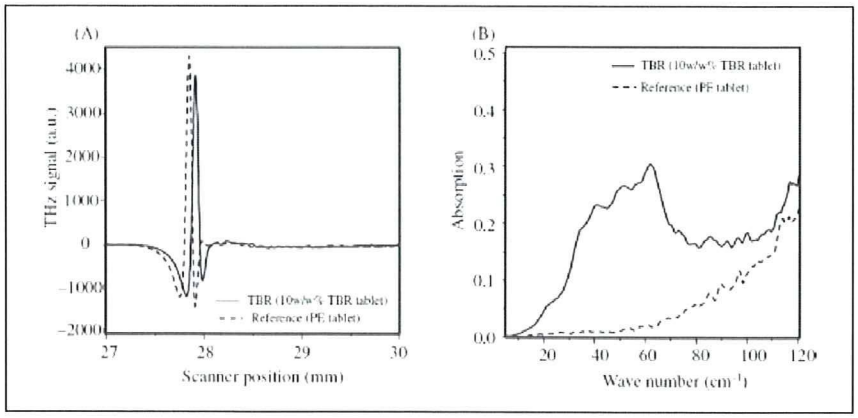

Fig. 1:
THz electric field records (A) and Fourier-transformed THz waveforms (B) of the TBR pellet and reference (PE pellet). The unique absorbance range, from 40 cm^{-1} to 70 cm^{-1}, is available to detect TBR absorbance

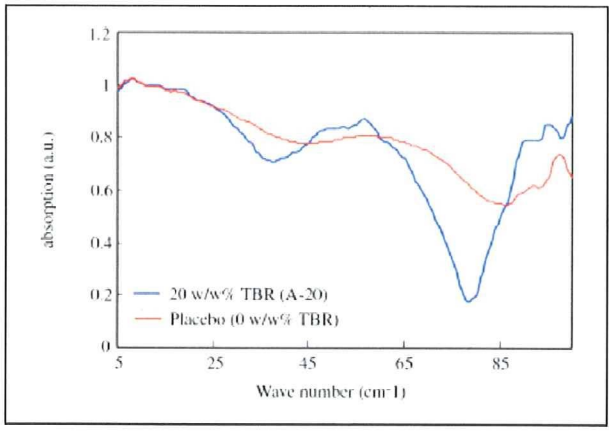

Fig. 2: THz spectra of model tape (20 w/w%, A-20) and placebo tape (0 w/w% TBR) obtained with quartz. The characteristic THz spectral range of TBR (from 45 cm^{-1} to 70 cm^{-1}) is best observed when etaloning effects are not dominating the range due to the thinness of the sample, as was the case here

the TPS 1000. The THz electric field record of the TBR pellet was shifted compared with that of the reference and the unique Fourier-transformed THz waveform of TBR was observed compared with that of the PE reference (Fig. 1(B)). This unique absorbance range, from 70 cm^{-1} to 45 cm^{-1}, seemed to be available to detect TBR absorbance from the total waveform of tapes.

2.2. THz image and spectra of TBR crystal in matrix

Fig. 2 shows the Fourier-transformed THz spectra of the placebo tape (the red line, an acrylic matrix) and the model tape (the blue line, 20w/w% TBR in an acrylic matrix, A-20). The fingerprint-like waveform of TBR from 70 cm^{-1} to 45 cm^{-1} was observed in the THz spectra obtained from the A-20. This observation suggests that chemical information of TBR can be detected in a tape. A lump of TBR crystals was detected at the top left of the image (Fig. 3(A)). The TPI contrast derives from refractive index differences. Therefore, it was presumed that the edge of the lumps of the TBR crystals contributed to making the definite contrast of shift of the refractive index. However, the image that is made from the shift of a refractive index would not provide chemical information about the lumps of TBR crystals. In order to identify the origin of the lumps of crystals, the THz spectra obtained from pixels which are located inside the lumps or outside the lumps were compared. Both spectra are shown in Fig. 3(B). The waveform indicated as the blue line represents the THz spectrum obtained from the pixel that is located inside the lump of crystals. The red line indicates the spectrum obtained from a pixel that is located outside the lump of crystals. The THz spectrum from the crystal shows a characteristic waveform range from 70 cm^{-1} to 45 cm^{-1}, almost the same as that of TBR standard substance. This observation strongly suggests that an image could be obtained from the crystal formed from TBR.

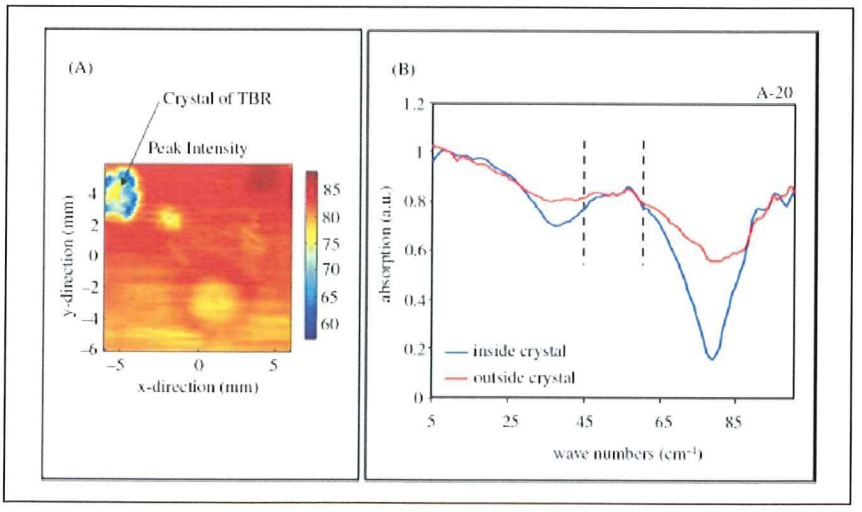

Fig. 3:
THz image of TBR crystal (A) and Fourier-transformed waveforms of pixels inside and outside of the crystals (B), obtained from A-20. The aggregation of TBR crystals which the arrow points to was clearly identified (A). It should be possible to observe the characteristic spectrum of TBR (from 45 cm^{-1} to 60 cm^{-1}) from both pixels located inside and outside of the crystal, but etaloning effects are again dominating the spectra

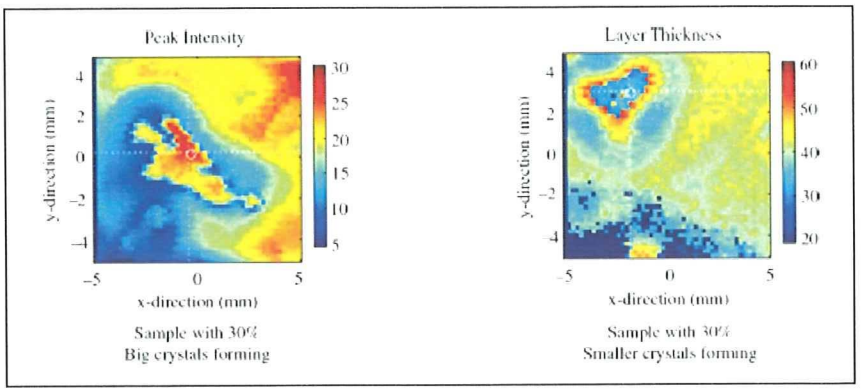

Fig. 4:
THz image of TBR crystals in matrix obtained using TPI 1000. Several sizes of TBR crystals were detected in the scanned area (the longer diameters: 0.5 mm to 3 mm, the shorter diameters: 0.1 mm to 0.2 mm)

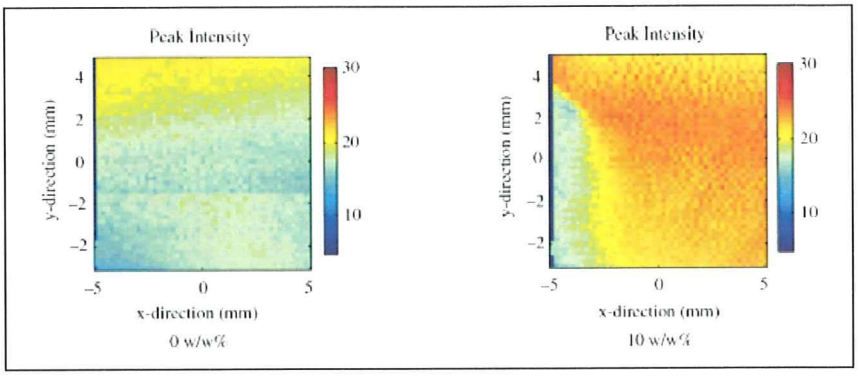

Fig. 5:
THz images of model tapes (0 and 10 w/w% TBR). Although there should be many small white crystals in R-10, only some were detected in the scanned area. In cases where the white crystals cannot be observed, the crystals might be smaller than the spatial resolution (100 μm) of TPI. Further studies need to be carried out to investigate differences in the samples

2.3. Size of crystals and spatial resolution of TPI

Fig. 4 shows the THz image obtained from the model tape (30 w/w% TBR, an acrylic matrix, A-30). Both model tapes were obtained from the same batch. Several sizes (short: 0.1 mm–0.2 mm, long: 0.5 mm–3 mm) of crystals were observed in these images.

The THz images obtained from the placebo tape (a rubber matrix, R-0) and the model tape (10 w/w% TBR, rubber matrix, R-10) are shown in Fig. 5. The image on the right side was obtained from R-10. Although small white crystals can be observed through a liner or a supporting board, no image of the lumps was observed in the THz image. This suggested that the sizes of the TBR crystals were smaller than the spatial resolution of TPI (approximately 100 μm). According to our study using Microscopic Laser Raman Spectroscopy/Mapping, the size of the TBR crystals was estimated to be from 6 μm to 40 μm (Sakamoto et al. 2006, 2007).

2.4. Depth image of crystals in TDDS tape

The THz image of A-30 and its depth image are shown in Fig. 6. The thickness of the lump of crystals in the matrix increased. The refractive index of the THz pulse was shifted due to the edges of the lumps of TBR crystals. This suggested that a comparatively big shift of a refractive index provides a definite image.

In conclusion, it was shown that THz spectroscopy/imaging technology was useful for detecting lumps of crystals of an active drug in transdermal tapes. THz spectroscopy/imaging can provide unique physical (and/or certain kinds of chemical) information compared with near infrared and/or mid infrared spectroscopy/imaging. In particular, obtaining a depth image from a pharmaceutical sample would be very useful for gaining an in-depth understanding of the quality of pharmaceuticals.

Although approximately 100 μm of spatial resolution in the THz pulsed image would hinder the detection of min-

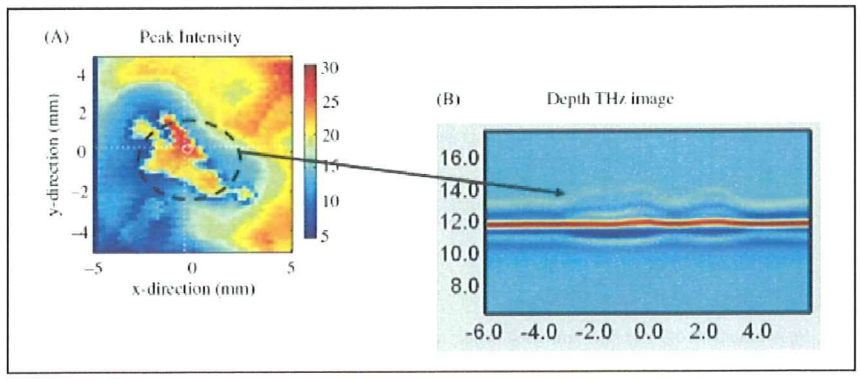

Fig. 6:
THz image of TBR crystal and depth THz image of matrix (A). The depth THz image in the scanned area where the crystal is observed shows the change in the thickness of the tape that can be seen (B)

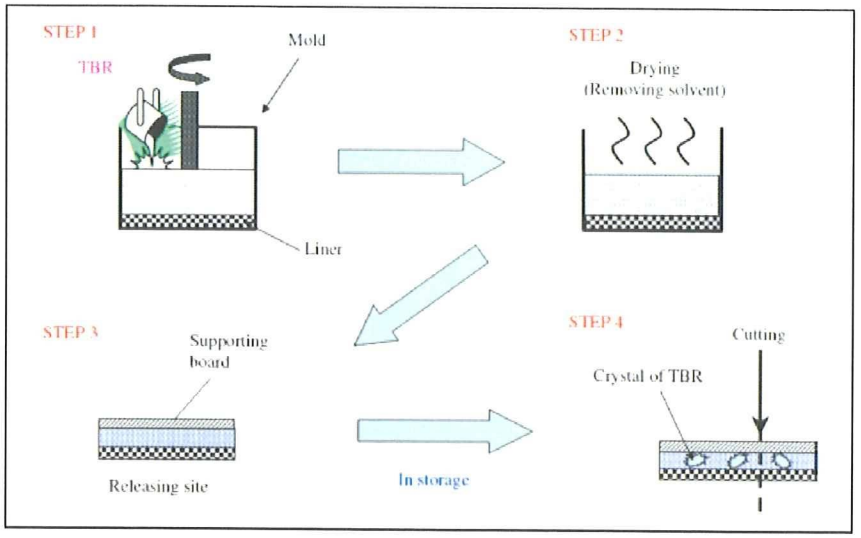

Fig. 7:
Flowchart showing preparation of model tapes. Residual solvents were removed by heating, and the mold was used to produce a sheet of model tape with a constant thickness and area

ute particles that are smaller than the spatial resolution, a reflective index of the THz pulsed wave may provide other useful information. Moreover, it would be able to detect problems caused by the manufacturing process, such as mixing of air bubbles and heterogeneity of active substances in the matrix. Therefore, this technology would be useful as an analytical tool not only for pharmaceutical quality control, but also for process control in pharmaceutical manufacturing.

Table: Prepared model transdermal tapes in this study

TBR level	Acrylic matrix	Rubber matrix
0 w/w% (Placebo)	A-0	R-0
10 w/w%	–	R-10
20 w/w%	A-20	–
30 w/w%	A-30	–

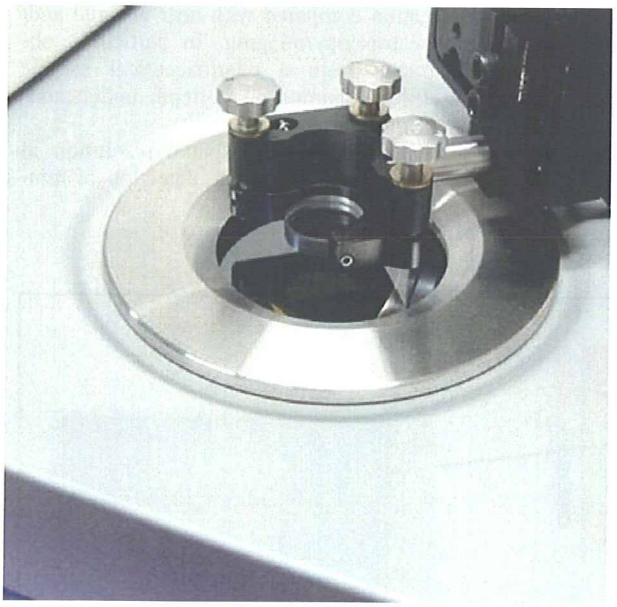

Fig. 8: Photograph of the metallic arm used when measuring the sample with a reference mirror

3. Experimental

3.1. Materials

TBR (purity > 99.0%) and model tapes were supplied by Hisamitsu Pharmaceutical Co Inc (Tokyo, Japan). Polyethylene (PE) powder of particle size < 80 μm was supplied by Induchem.

3.2. Model tapes

The model tapes were prepared by TDDS Laboratory, Hisamitsu Pharmaceutical Co Inc (Tsukuba, Japan). In order to identify crystals of TBR in the matrix, two kinds of matrices, rubber and acrylic matrices, were prepared. The flowchart for preparing the model tapes is shown in Fig. 7. TBR and other ingredients of the adhesive solutions were stirred in the mold adequately. The mixture was extended on the liner and residual solvents were removed by drying. When the thickness of the matrix (the adhesive layer) became a constant (approximately 50 μm thickness), a supporting board was pasted on the matrix after removing the mold. A polyethylene terephthalate (PET) film was selected as a liner and as a supporting board, for both the model and the placebo tape. And then these tapes cut to a size of 36 mm diameter. TBR crystals in model tapes were generated by leaving the tapes to crystallize for some time.
The model tape that contained 0 w/w% (R-0, placebo), 5 w/w% (R-5) or 10 w/w% (R-10) of TBR in a rubber matrix consisted of polyisobutylene, polybutene and lipocyclic petroleum resin. Small white crystals were seen in all areas of the matrix in the A-10 through a liner or a supporting board. The model tape that contained 0 w/w% (A-0, placebo), 20 w/w% (A-20) or 30 w/w% (A-30) of TBR in an acrylic matrix consisted of acryl adhesion polymer and isopropyl myristate. On the A-30 samples, small white crystals were seen in all areas of the matrices. A higher TBR concentration was needed to generate the crystals in the acrylic matrix compared with the rubber matrix because of the solubility of TBR. The prepared model tapes are shown in the Table.

3.3. Apparatus and measurements

3.3.1. Transmittance measurement of tablet by TPS

In order to identify a THz spectrum of TBR, a pellet containing approximately 10 w/w% of TBR was prepared by compressing at 2 t for 3 min with a press machine. The pellet was measured using a TPS 1000 spectrometer (TeraView Limited, Cambridge, UK). Each sample was measured covering the spectral range from 120 cm^{-1} to 2 cm^{-1} at 1.5 cm^{-1} of spectral resolution. Spectra were obtained averaging 1800 scans.

3.3.2. Transmittance-reflectance measurements of tapes by TPI

A reference mirror was first measured, and then the samples were mounted to the mirror and adjusted horizontally against the measurement window of the TPI Imaga^{TM} 1000 instrument (Fig. 8); subsequently, THz radiation was focused onto the samples to gain maximum sensitivity. Placebo tapes were used as a background for all measurements.
A TPI imaging system, TPI Imaga 1000 (TeraView Ltd., Cambridge, UK), was used for the reflectance measurement, which was operated in the rapid scan mode. Terahertz images were obtained by raster scanning the terahertz beam across the sample, which was mounted at the focus position. The scanned area was 12 mm × 12 mm, which corresponds to 120 pixels × 120 pixels at 100 μm spatial resolution. The total measurement time was approximately 30 min.

Acknowledgement: This study was supported in part by a research grant from the Ministry of Health, Labour and Welfare of Japan (H17-iyaku-ippan-040).

References

Day GM, Zeitler JA, Jones W, Rades T, Taday PF (2006) Understanding the influence of polymorphism on phonon spectra: Lattice dynamics calculations and terahertz spectroscopy of carbamazepine. J Phys Chem B 110: 447–456.

Fitzgerald AJ, Cole BE, Taday PF (2005) Nondestructive analysis of tablet coating thicknesses using terahertz pulsed imaging. J Pharm Sci 94: 177–183.

Ho L, Müller R, Römer M, Gordon KC, Heinämäki J, Kleinebudde P, Pepper M, Rades T, Shen YC, Strachan CJ, Taday PF, Zeitler JA (2007) Analysis of sustained-release tablet film coats using terahertz pulsed imaging. J Control Release 119: 253–261.

Sakamoto T, Fujimaki Y, Hiyama Y (2007) Study on development of quality analytical method using spectroscopic and imaging technique I. Application of Raman spectroscopy and mapping microscopy for quality evaluation of TDDS and Granules formulations. PharmTech Japan 23: 27–36 (in Japanese).

Sakamoto T, Matsubara T, Sasakura D, Takada Y, Fujimaki Y, Aida K, Miura T, Terahara T, Higo N, Kawanishi T, Hiyama Y (2009) Chemical mapping of tulobuterol in transdermal tapes using Microscopic Laser Raman Spectroscopy. Pharmazie 64: 166–171.

Strachan CJ, Taday PF, Newnham DA, Gordon KC, Zeitler JA, Pepper M, Rades T (2005) Using terahertz pulsed spectroscopy to quantify pharmaceutical polymorphism and crystallinity. J Pharm Sci 94: 837–846.

Strachan CJ, Rides T, Newnham DA, Gordon KC, Pepper M, Taday PF (2004) Using terahertz pulsed spectroscopy to study crystallinity of pharmaceutical materials. Chem Phys Lett 390: 20–24.

Taday PF, Bradley IV, Arnone DD, Pepper M (2003) Using terahertz pulse spectroscopy to study the crystalline structure of a drug: a case study of the polymorphs of ranitidine hydrochloride. J Pharm Sci 92: 831–838.

Ueno Y, Rungsawang R, Tomita I, Ajito K (2006) Quantitative measurements of amino acids by terahertz time-domain transmission spectroscopy. Anal Chem 78: 5424–5428.

Upadhya PC, Shen YC, Davies AG, Linfield EH (2003) Terahertz time-domain spectroscopy of glucose and uric acid. J Biol Phys 29: 117–121.

Walther M, Fischer BM, Jepsen PU (2003) Noncovalent intermolecular forces in polycrystalline and amorphous saccharides in the far infrared. Chem Phys 288: 261–268.

Zeitler JA, Newnham DA, Taday PF, Strachan CJ, Pepper M, Gordon KC, Rades T (2005) Temperature dependent terahertz pulsed spectroscopy of carbamazepine. Thermochim Acta 436: 70–76.

Zeitler JA, Shen YC, Baker C, Taday PF, Pepper M, Rades T (2006) Analysis of coating structure and interfaces in solid oral dosage forms by three dimensional terahertz pulsed imaging. J Pharm Sci 96: 330–340.

Zeitler JA, Newnham DA, Taday PF, Threlfall TL, Lancaster RW, Berg RW, Strachan CJ, Pepper M, Gordon KC, Rades T (2006) Characterization of temperature-induced phase transitions in the five polymorphic forms of sulfathiazole by terahertz pulsed spectroscopy and differential scanning calorimetry. J Pharm Sci 95: 2486–2498.

Zeitler JA, Taday PF, Pepper M, Rades T (2007) Relaxation and crystallization of amorphous carbamazepine studied by terahertz pulsed spectroscopy. J Pharm Sci 96: 2703–2709.

Malaysian Journal of Chemistry, 2009, Vol. 11, No. 1,088 - 093

Chiral Analysis of Re-crystallized Mixtures of D-, L-amino Acid Using Terahertz Spectroscopy

Tomoaki Sakamoto[1], Tadao Tanabe[2], Tetsuo Sasaki[3], Yutaka Oyama[2], Jun-ichi Nishizawa[3], Toru Kawanishi[1], Yukio Hiyama[1]

[1]Division of Drugs, National Institute of Health Sciences, Tokyo 158-8501, Japan
[2]Graduate School of Engineering, Tohoku University, Sendai 980-8579, Japan
[3]Center for Priority Area, Tokyo Metropolitan University, Tokyo 192-0397, Japan
Corresponding author email address: tsakamot@nihs.go.jp

Abstract: Distinguishability by terahertz absorption between D- and L-amino acids and a change in terahertz absorption based on the re-crystallization condition was examined. Terahertz spectra which were obtained from the re-crystallized each enantiomer or mixtures of D- and L-leucine or alanine were compared with those of the purchased reagents. The peak tops of the re-crystallized L- and D-leucine mixtures were shifted toward low frequency side and the half width of the peak at 3.7 THz became narrow to approximately half of that of the reagent. Difference of spectral features from 2.1 THz to 2.8 THz in the THz spectra between D- and L-alanines was observed. According to the result of peak separation against these spectra, distinction between the purchased D- and L-alanine was possible to compare the intensities of the sub-peaks. Moreover, changes of the integrated values of the peaks obtained from L- or D-form-rich mixture of leucine were observed. These results suggested that feasibility of chiral analysis of enantiomers using terahertz spectroscopy would be shown.

Keywords: Terahertz spectroscopy, polymorphs, enantiomers, crystals

Introduction

Terahertz (THz) electro-magnetic region (0.1 THz to 10 THz, 3.3 cm^{-1} to 333 cm^{-1}) detects a weak inter-molecular energy such as a hydrogen bond, and a crystal lattice vibration. In the pharmaceutical and the chemical industries, detection of polymorphs (1-8) and unique THz spectra obtained from active pharmaceutical ingredients (APIs), illegal drugs and explosives have been reported (1, 3, 6). The hydrogen bond and van der Waals force, which contribute to form the function-able structure of protein and amino acids, would be sensitively detected in THz region. Thus, absorption on THz electro-magnetic region would be expected to provide useful information for investigation of the function and the dynamics of these compounds. Amino acids which are components of protein are used as not only a supplement for keeping health but also a medication for certain diseases. Amino acids have hydrogen bond network in their crystals. Thus, an investigation concerning property of hydrogen bonds and intermolecular interactions would be useful to understand the functions of these compounds. Moreover, amino acids exist as L-form in nature, and their biological function is different by stereo- configuration. In study about an optical isomerism by THz spectroscopy, distinction between racemate and enantiomer by THz peaks has been reported (9, 10). However, distinguishability between both enantiomers has not been established yet. The authors examined the THz spectral change of the re-crystallized amino acids, leucine and alanine using THz electro-magnetic wave.

Materials and Methods

L-, D- and DL-leucine (racemate), and L-, D-, and DL-alanine (racemate) were purchased from Wako Pure Chemical Industries, Ltd. (Osaka, Japan). Polyethylene powder for making pellets was purchased from THz Laboratory Co., Ltd. (Akita, Japan).

Re-crystallization of these compounds was performed with water. Sample powder was dissolved in water at around 90 °C and cooled down to room temperature. Then, this solution was put into a refrigerator at 4 °C. Re-crystallized sample was filtered and washed with iced water, and dried in a desiccator under reduced pressure. The mixture of L- and D-amino acids which contains 25 % or 75 % of L-enantiomer was re-crystallized to make D- or L-form-rich mixed sample. The re-crystallized sample was diluted to concentration of 0.25 mol/l with polyethylene powder and then the mixture was compressed at 9.8 kN for 2 min to make pellets for transmittance measurements.

Measurements of THz spectra were performed by the Gallium-Phosphorus (GaP) THz signal generator system equipped with a pyroelectric DTGS detector. This THz generator system has been developed and constructed by Nishizawa et al (11-19). The optical system of this instrument is shown in Fig. 1. The spectra were measured from 1 THz (33 cm^{-1}) to 5 THz (167 cm^{-1}) at 15 GHz measurement steps. Measurements of optical rotations of the re-crystallized D-, L-amino acids and their mixtures were performed using DIP-360 polarimeter (JASCO, Tokyo, Japan).

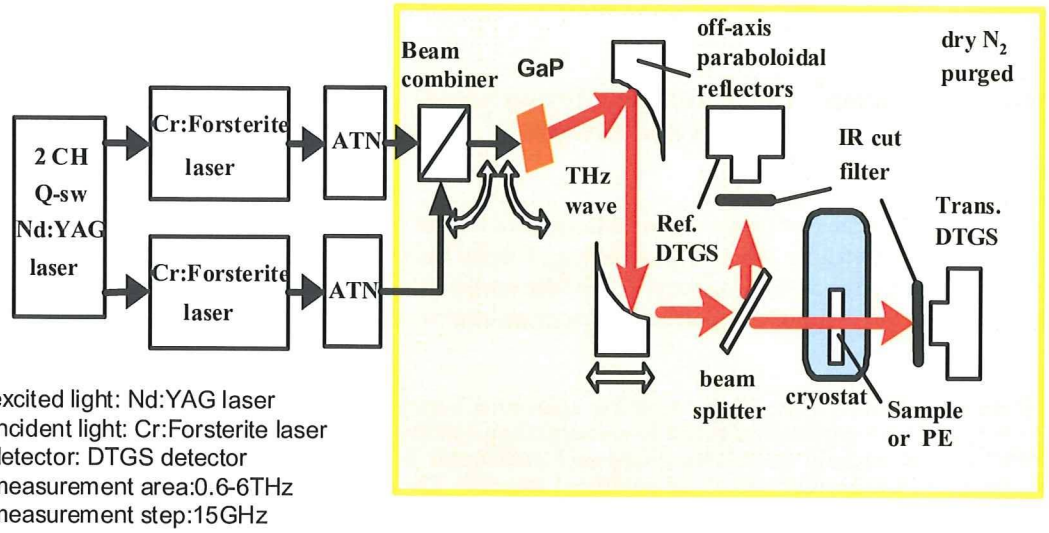

Figure 1: Schematic diagram of GaP-THz spectrometer via differential frequency generation

Results and Discussion

The baseline corrected THz spectra obtained from the purchased D-, L-, and leucine racemate are shown in Fig. 2(A). The peak at 3.7 THz was observed in both enantiomers. However, this single peak was shifted to 3.6 THz in racemate and the half width of the peak height of the enantiomers (0.7 THz) was narrowed to 0.4 THz. The baseline corrected THz spectra obtained from the re-crystallized mixtures are shown in Fig. 2(B). The intensity (a relative absorption coefficient) of D-leucine was approximately 20 % higher than that of DL-leucine. On the other hand, L-leucine showed 20 % lower intensity than that of racemate. No significant difference was observed about the waveforms, the peak position, and the half width of peak height at 3.7 THz between D- and L-leucine. In case of the mixtures, the peak positions were shifted to lower side of frequency, and the half width of peak height at 3.7 THz also became narrow as well as the purchased leucines. In order to investigate the THz peaks, the peak separation by Gaussian function was carried out. The single peak at 3.7 THz was separated to one main peak and 2 sub-peaks. Figure 3 shows the correlations between the spiked amount of L-form and the peak positions or the integrated values of peaks. Although the peak positions of the main peak were same in all mixtures, the peak positions of the sub-peaks of L- or D-form-rich mixture came up to that of the racemate. These results suggest that the existence of the other enantiomer would affect the phonon of crystallized leucine molecules. On the other hand, the correlation between the integrated values and the spiked amount of L-leucine shows the integrated values of the main peak were smallest on the D- or L-form-rich mixture resulting in a W-like pattern. The highest integrated value of the low sub-peak was observed in the D- or L-form-rich mixture, and shows an inverted W-like pattern. Moreover, the integrated value of L-leucine was comparatively higher than that of D-leucine. The peak integrated value of D-form-rich mixture of the high sub-peak was small, but it became bigger as the D-form content was increased. Furthermore, the integrated value in L-enantiomer remarkably increased and the value doubled compared with that of D-enantiomer. These results suggest that those values of D- or L-leucine were influenced by the existence of the other enantiomer, and the value of the high sub-peak at 4.1THz had correlated with the spiked content of D- or L-leucine in the re-crystallized mixture. The baseline corrected THz spectra obtained from the purchased D-, L-, and DL-alanine (Racemate) are shown in Fig. 4(A). Each optical isomer shows 2 peaks at 3.2 THz and 3.4 THz, racemate has the single peak at 3.1 THz. After re-crystallization, the two peaks on the THz waveform on D- or L-enantiomer were shifted to 4.2 THz and 4.4 THz. Moreover, the single peak of racemate was shifted to 4.1 THz on the THz wave obtained from L-form-rich or D-form-rich mixture (Fig. 4(B)). These results suggest that crystalline forms were changed from those of the purchased alanines because the distributor of these reagents would have done a different purification process from the re-crystallization method which was used in this study. In the THz waveform of the re-crystallized racemate, an increase of the relative molar absorbance was observed as the spiked content of D-enantiomer increased. In the THz waveform obtained from the purchased D- and L-alanine, small differences were observed at the frequency range from 2.1 THz to 2.8 THz.

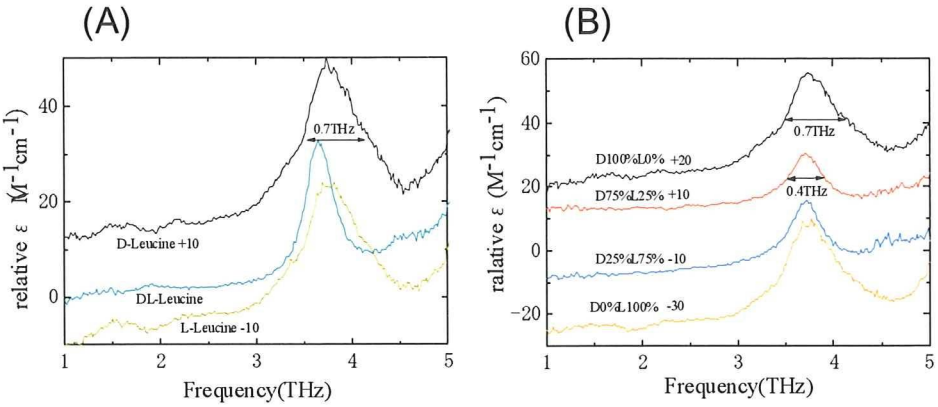

Figure 2: THz spectra of leucines (A: D-, L-, and DL-leucine (racemate) as purchased B: four kinds of re-crystallized D- and L-mixture)

In order to characterize the small differences, the curve separation was employed. Figure 5 shows the calculated D- and L-alanine waveforms by the Gaussian function. The three main peaks at 2.25 THz (No.1), 2.45 THz (No.2) and 2.6 THz (No.3) and the sub-peak at 2.7 THz (C) were calculated from the waveform of D-enantiomer. In case of L-enantiomer, the intensity of the peak No.2 became smaller compared with that of D-enantiomer. Moreover the two sub-peaks at 2.2 THz and 2.35 THz appeared and then the sub-peak C which was observed in D-enantiomer disappeared. While no significant differences between both enantiomers about the peak positions and the integrated values of peaks were observed, the peak intensities at the peak No.2 and No.3 of L-enantiomer were smaller than D-enantiomer. Although further study is necessary to explain the detail of these observations, the purchased D- and L-alanine may be distinguishable using THz spectroscopy.

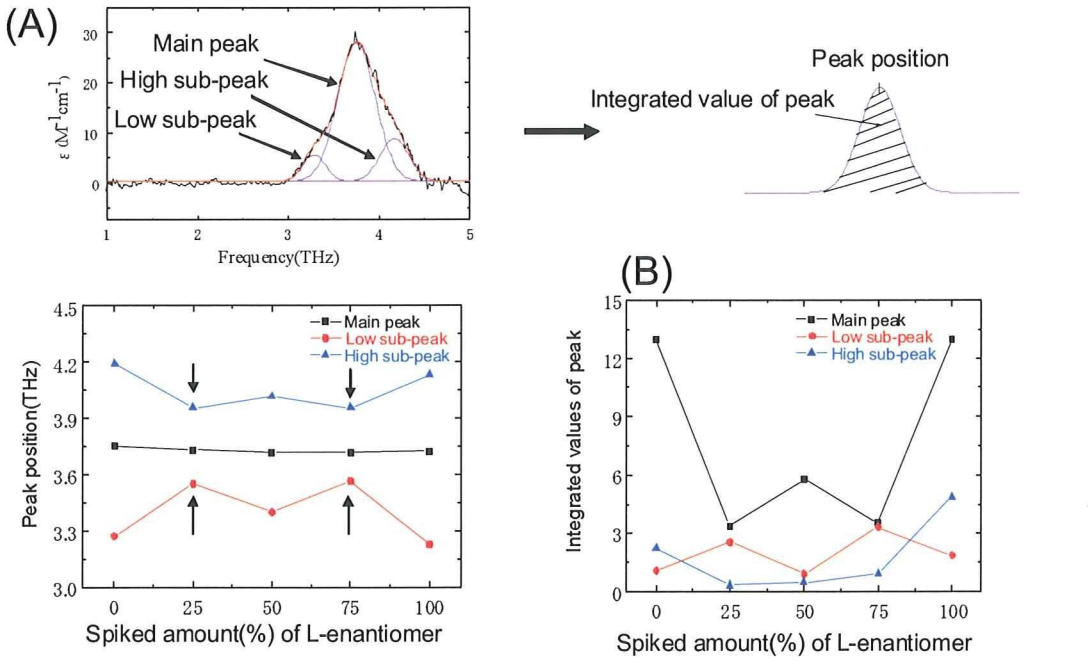

Figure 3: Correlations between re-crystallized mixtures and THz peaks (A: Peak positions (THz), B: Integrated values of peaks)

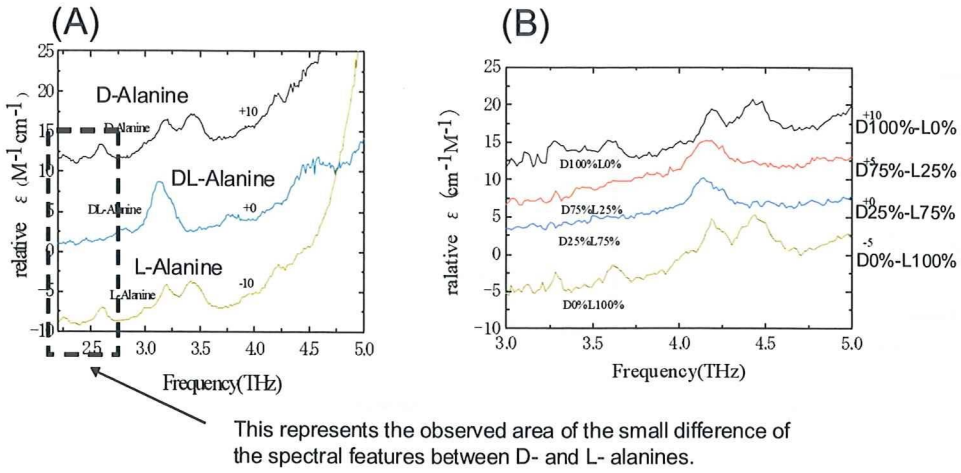

Figure 4: THz spectra of alanines (A: D-, L-, and DL-alanine (racemate) as purchased B: four kinds of re-crystallized D- and L-mixture)

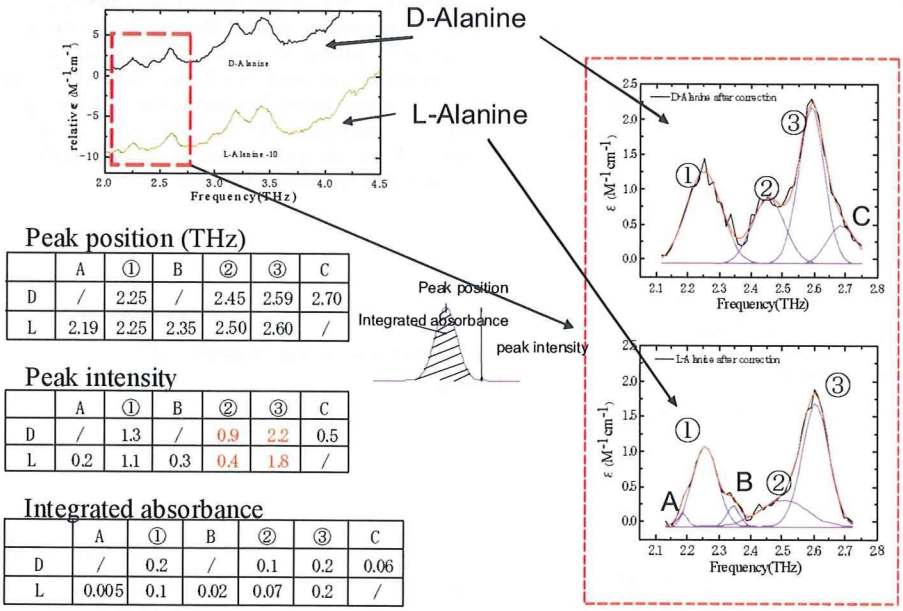

Peak position (THz)

	A	①	B	②	③	C
D	/	2.25	/	2.45	2.59	2.70
L	2.19	2.25	2.35	2.50	2.60	/

Peak intensity

	A	①	B	②	③	C
D	/	1.3	/	0.9	2.2	0.5
L	0.2	1.1	0.3	0.4	1.8	/

Integrated absorbance

	A	①	B	②	③	C
D	/	0.2	/	0.1	0.2	0.06
L	0.005	0.1	0.02	0.07	0.2	/

Figure 5: Fitted THz peaks of alanine and calculation results of three evaluation parameters

While comparative large two peaks (from 4.1 THz to 4.6 THz) were observed in D- or L-leucine, only single peak was detected in racemate and the re-crystallized mixtures. The authors are thinking that a hydrogen bond network of racemate which has a crystal structure formed by distributing of D- and L-enantiomer alternately is different from a hydrogen bond network in a crystal structure of each enantiomer. For example, a hydrogen network in three-dimensional structure of D- or L-enantiomer can be illustrated as Fig. 6 based on the crystalline structure of L-enantiomer (20).

On the other hand, a hydrogen bond network of racemate is formed by distributing both enantiomers alternately. Then a single molecule in crystal formed from D- or L-form molecule may construct a hydrogen bond network ([-O --- H-N-]) between adjacent two molecules. In case of racemate, D- or L-form molecule may construct two hydrogen networks between the other L- and D-form molecules (Fig. 7). The authors predict that inter-molecular vibration modes detected in THz spectra are correlated with an infra-red activity mode. Symmetry of crystal structure between enantiomer and racemate is different. Then, an infra-red active inter-molecular mode in enantiomer might change into an inactive mode in racemate. And

the opposite changing may be also observed. Of course further investigation is necessary to test this hypothesis; a difference of configuration to take high-density and/or stable crystal structure may affect THz spectral features.

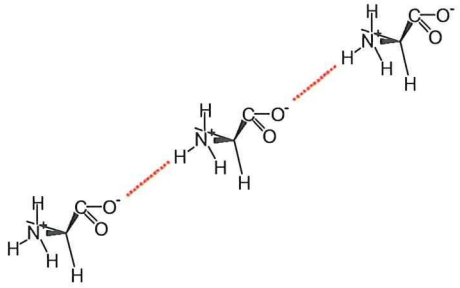

Figure 6: The image of a hydrogen bond between L-leucine and an adjacent one (Only one hydrogen bond is shown here.)

The different spectral feature between D- and L-alanine was observed in the range from 2.1 THz to 2.8 THz. In the calculated three peaks, the intensity of the peak No.2 was significantly decreased. Moreover, different calculated sub-peaks pattern between D- and L-enantiomer was observed as described in the paragraph 3.2. D- and L-enantiomer has the identical physical properties except an optical rotation. Although there is a possibility that an impurity derived from a different purification process between D- and L-leucine may cause spectral differences, it also has possibility that THz spectroscopy can sensitively detect small differences concerning a hydrogen bond network or a crystal lattice vibration.

A difference of spectral features between D- and L-leucine was not observed, but the differences of the integrated values of the peaks (shown in Fig. 5) obtained from the two sub-peaks between racemate and L- or D-form-rich mixture were observed. The optical rotation of re-crystallized mixture, L0%-D100%, L25%-D75%, L50%-D50%, L75%-D25% and L100%-D0% were -15.74 ± 0.02°, -0.06 ± 0.01°, 0.10 ± 0.02°, 0.12 ± 0.01° and 15.58 ± 0.01°, respectively. An isomerization in the aqueous solution and a thermo-isomerization of enantiomer was not observed. According to these results, According to these results, these re-crystallized mixtures did not include whole spiked amounts of L- or D-enantiomer. Most of these mixtures were formed by racemate, and a portion of excess L- or D-enantiomer was distributed in these crystals. Furthermore, no significant difference of the optical rotation between L50% and L75% mixtures was calculated. Thus, it is presumed that a racemization of D- and L-leucines in the solution was first progressed and then a portion of excess D- or L-enantiomer was taken in the racemate crystals. Although investigation of crystal structure of these mixtures is necessary to explain this observation, each D- or L-form-rich mixture showed the characteristic THz spectral features.

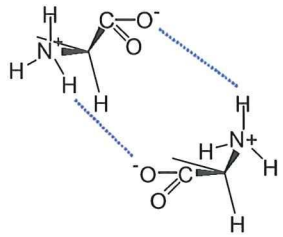

Figure 7: The image of assumed hydrogen bonds between two adjacent molecules in racemate

Conclusion

In this study, distinguishability of chiral compounds by THz spectroscopy was examined. Characteristic spectral differences between enantiomers and mixtures were observed by detailed analysis of spectral features. Because THz electro-magnetic wave can detect small but meaningful differences of crystal structure, more applications of THz electro-magnetic wave to analyze and to evaluate crystalline state and physical properties will be expected in the future.

Acknowledgement

This study was supported in part by a research grant from the Ministry of Health, Labour and Welfare of Japan (H20-iyaku-ippan-004).

References

1. P.F. Taday, I.V. Bradley, D.D. Arnone, M. Pepper, (2003) Using terahertz pulse spectroscopy to study the crystalline structure of a drug: a case study of the polymorphs of ranitidine hydrochloride, *J. Pharm.Sci.,* **92,** 831-838
2. M. Walther, B.M. Fischer, P.U. Jepsen (2003), Noncovalent intermolecular forces in polycrystalline and amorphous saccharides in the far infrared, *Chem. Phys.,* **288,** 261-268
3. C.J. Strachan, T. Rides, D.A. Newnham, K.C. Gordon, M. pepper, P.F. Taday, (2004) Using terahertz pulsed spectroscopy to study crystallinity of pharmaceutical materials, *Chem. Phys. Lett.*, **390,** 20-24
4. J.A. Zeitler, D.A. Newnham, P.F. Taday, T.L. Threlfall, R.W. Lancaster, R.W. Berg, C.J. Strachan, M. Pepper, K.C. Gordon, T. Rades, (2006) Characterization of temperature induced phase transitions in the five polymorphic forms of sulfathiazole by terahertz pulsed spectroscopy and differential scanning calorimetry, *J. Pharm. Sci.,* **95,** 2486-2498
5. J.A. Zeitler, D.A. Newnham, P.F. Taday, C.J. Strachan, M. Pepper, K.C. Gordon, T. Rades, (2005) Temperature dependent terahertz pulsed spectroscopy of carbamazepine, *Thermochimica Acta,* **436**, 70-76
6. C.J. Strachan, P.F. Taday, D.A. Newnham, K.C. Gordon, J.A. Zeitler, M. Pepper, T. Rades, (2005) Using terahertz pulsed spectroscopy to quantify pharmaceutical polymorphism and crystallinity, *J. Pharm. Sci.*, **94**, 837-846
7. G.M. Day, J.A. Zeitler, W. Jones, T. Rades, P.F. Taday, (2006) Understanding the influence of

polymorphism on phonon spectra: Lattice dynamics calculations and terahertz spectroscopy of carbamazepine, *J. Phys. Chem. B*, **110,** 447-456

8. J.A. Zeitler, P.F. Taday, M. Pepper, T. Rades, (2007) Relaxation and crystallization of amorphous carbamazepine studied by terahertz pulsed spectroscopy, *J. Pharm. Sci.,* **96**, 2703-2709
9. M. Yamaguchi, F. Miyamaru, K. Yamamoto, M. Tani and M. Hangyo, (2005) Terahertz absorption spectra of L-, D-, and DL-alanine and their application to determination of enantiometric composition, *Appl. Phys. Lett.,* **86**, 053903-1-3
10. R. Nishikiori, M. Yamaguchi, K. Takano, T. Enatzu, M. Tani, U. Chandimal de Silva, N. Kawashita, T. Takagi, S. Morimoto, M. Hangyo and M. Kawase, (2008) Application of Partial Least Square on quantitative analysis of L-, D, and DL-tartaric acid by terahertz absorption spectra, *Chem. Pharm. Bull*, **56**, 305-307
11. T. Tanabe, K. Suto, J. Nishizawa, T. Kimura, K. Saito, (2003) Frequency tunable high power terahertz wave generation from GaP, *J. Appl. Physics*, **93,** 4610-4615
12. T. Tanabe, K. Suto, J. Nishizawa, K. Saito, T. Kimura, (2003) Frequency-tunable terahertz wave generation via excitation of phonon-polaritons in Ga, *J. Physics D: Appl. Physics,* **36,** 953-957
13. T. Tanabe, K. Suto, J. Nishizawa, K. Saito, T. Kimura, (2003) Tunable terahertz wave generation in the 3- to 7-THz region from GaP, *Appl. Physics letters*, **83**, 237-239
14. T. Tanabe, Y. Kozawa, K. Suto, J. Nishizawa, Y. Oyama, (2005) Observing the stimulated Raman gain spectra of solutions using an infrared pump pulse with narrow linewidth and a low-noise cw probe laser, *Int. J. Infrared and Millimeter Waves,* **26,** 881-892
15. J. Nishizawa, T. Sasaki, K. Suto, T. Tanabe, K. Saito, T. Yamada, T. Kimura, (2005) THz transmittance measurements of nucleobases and related molecules in the 0.4 to 5.8THz region using a GaP THz wave generator, *Optics Comminications*, **246**, 229-239
16. J. Nishizawa, T. Sasaki, K. Suto, T. Yamada, T. Tanabe, T. Tanno, T. Sawai and Y. Miura, (2005) THz imaging of nucleobases and cancerous tissue using a GaP THz-wave generator, *Optics Comminications,* **244**, 469-274
17. J. Nishizawa, T. Sasaki, K. Suto, T. Tanabe, T. Yoshida, T. Kimura and K. Saito, (2006) Frequency-Tunable terahertz-wave generation from GaP using Cr:Forsterite lasers, *Int. J. Infrared and Millimeter Waves,* **27,** 779-789
18. T. Tanabe, J. Nishizawa, K. Suto, Y. Watanabe, T. Sasaki, Y. Oyama, (2007)Terahertz wave generation from GaP with continuous wave and pulse pumping in the 1-1.2μm region, *Materials Transactions,* **48**, 980-983
19. J. Nishizawa, T. Sasaki, K. Suto, M.Ito, T. Yoshida, T. Tanabe, (2008) High-resolution GaP terahertz spectrometer and its application to detect defects in γ-irradiated glucose crystal, *Int. J. Infrared and Millimeter Waves,* **29,** 291-297
20. A.R. Taulbee, J.A. Heuser, W.U. Spendel and G.E. Pacey, (2009) Qualitative analysis of collective mode frequency shifts in L-alanine using terahertz spectroscopy, *Anal. Chem.,* 2664-2667